BNL-211775-2019-JAAM

Onsurface synthesis and spectroscopic characterization of laterally extended chevron graphene nanoribbons

J. D. Teeter, P. Zahl

To be published in "ChemPhysChem"

June 2019

Center for Functional Nanomaterials

Brookhaven National Laboratory

U.S. Department of Energy

USDOE Office of Science (SC), Basic Energy Sciences (BES) (SC-22)

DISCLAIMER

On-surface synthesis and spectroscopic characterization of laterally extended chevron graphene nanoribbons

Jacob D. Teeter,[a] Percy Zahl,[b] Mohammad Mehdi Pour,[a] Paulo S. Costa,[c] Axel Enders,[c,d,e] Alexander Sinitskii*[a,e]

We report the on-surface synthesis and spectroscopic study of laterally extended chevron graphene nanoribbons (GNRs) and compare them with the established chevron GNRs, emphasizing the consistency of bandgap reduction of semiconducting GNRs with increased width. The extended chevron GNRs grown on Au(111) exhibit a bandgap of about 2.2 eV, which is considerably smaller than the values reported for chevron GNRs in similar studies.

Graphene nanoribbons (GNRs) attract a great deal of attention because of their highly tunable electronic properties and potential for numerous applications in electronics,[1] spintronics,[2] photovoltaics[3, 4] and gas sensors.[5] It is well established that the properties of GNRs strongly depend on their structural parameters, such as width, edge type and chemical functionalization.[6-10] A precise control over these parameters enables realization of a variety of interesting physical properties, which include a highly tunable energy bandgap,[6-8] edge magnetism[2, 9, 10] and topological electronic states.[11] While several kinds of atomically precise GNRs have been demonstrated in recent years,[12, 13] there is a great interest in the synthesis and electronic characterization of new atomically precise GNRs which expand the repertoire of available nanoribbons and often provide experimental verification for theoretically predicted phenomena.[14-18]

A variety of atomically precise GNRs can be synthesized by the on-surface approach pioneered by Cai *et al.*,[19] which is based on the coupling of halogenated molecular precursors on metal substrates and subsequent cyclodehydrogenation of the resulting polymers at elevated temperatures. One of the ribbons demonstrated in the original study by Cai *et al.* is the chevron GNR (cGNR) shown in Fig. 1a.[19] This nanoribbon can be prepared by deposition of 6,11-dibromo-1,2,3,4-tetraphenyltriphenylene on Au(111) in ultrahigh vacuum (UHV), annealing at about 200 °C to promote on-surface polymerization and further annealing of the resulting polymer at about 440 °C to initiate its cyclodehydrogenation and the formation of cGNR.[19]

Since then, a considerable number of studies have been dedicated to the synthesis and characterization of cGNRs and structurally related nanoribbons.[20-33] In addition to the original demonstration of the cGNR growth on Au(111),[19] chevron GNRs have been also prepared on Cu(111)[20] and synthesized by an alternative solution polymerization approach,[21, 22] doped with heteroatoms[23-29] and modified with functional groups,[30, 31] and have even become the basis for the GNR cross-junctions[32] and heterojunctions.[26, 27, 30, 33]

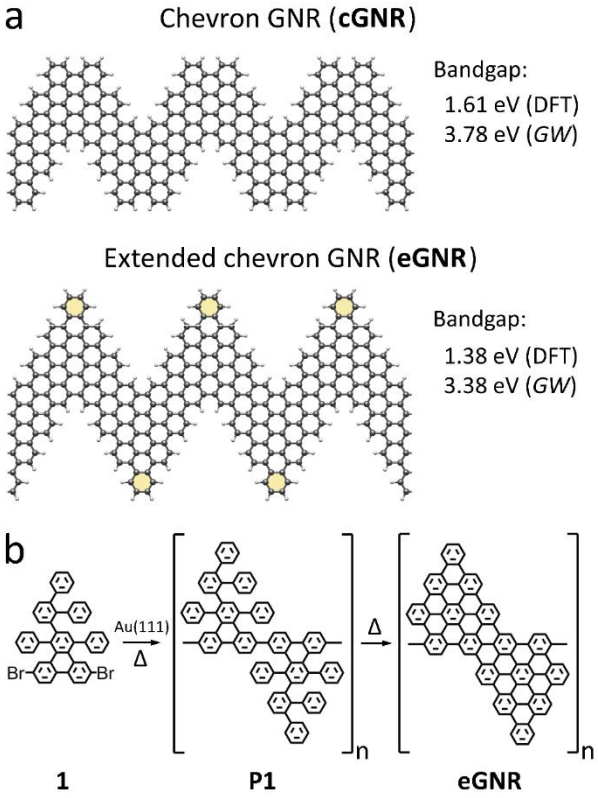

Figure 1. Synthesis of eGNRs. (a) Fragments of a cGNR and an eGNR; large spheres – carbon atoms, small spheres at the edges – hydrogen atoms. eGNRs can be viewed as cGNRs with extra benzene rings (highlighted by yellow) in the convex regions. The bandgap values are from ref. [5]. (b) Scheme of the on-surface synthesis of eGNRs.

While chevron GNRs have been extensively studied over the last few years, much less is known about another nanoribbon shown in Fig. 1a, which is structurally related to the cGNR and will be referred to as a laterally extended chevron GNR (eGNR).[5] Compared to the cGNR, the eGNR has an additional benzene ring in each convex region, as shown in Fig. 1a. The synthesis of

[a] J. D. Teeter, Prof. Alexander Sinitskii
Department of Chemistry, University of Nebraska – Lincoln, Lincoln, NE 68588, USA
E-mail: sinitskii@unl.edu
[b] Dr. P. Zahl
Center for Functional Nanomaterials, Brookhaven National Laboratory, Upton, NY 11973, USA
[c] Dr. P. S. Costa, Prof. Axel Enders
Department of Physics and Astronomy, University of Nebraska – Lincoln, Lincoln, NE 68588, USA
[d] Prof. Axel Enders
Physikalisches Institut, Universität Bayreuth, Bayreuth, 95440, Germany
[e] Prof. Axel Enders, Prof. Alexander Sinitskii
Nebraska Center for Materials and Nanoscience, University of Nebraska – Lincoln, Lincoln, NE 68588, USA

eGNRs was first performed in solution by Ni^0-mediated Yamamoto polymerization of 2-([1,1':2',1"-terphenyl]-3'-yl)-6,11-dibromo-1,4-diphenyltriphenylene (molecule **1**; see Fig. 1b) followed by the oxidative cyclodehydrogenation of the resulting polymer *via* the Scholl reaction using iron(III) chloride.[5] While the molecule 1 is not symmetrical relative to the plane perpendicular to the polymerization direction, both possible orientations of the monomer behave identically with respect to the polymerization reaction, as it is directed by the radicals resulting from dehalogenation and is thus unaffected by substituents in other positions. It has been experimentally demonstrated that eGNRs possess promising gas sensing properties[5] and can be combined with cGNRs in graphene nanoribbon heterojunctions.[33] However, there has been no study focused exclusively on the on-surface synthesis of eGNRs. In particular, there has been no spectroscopic characterization of eGNRs on Au(111), which would allow comparison of their bandgap with those of other GNRs that have been predominantly studied on Au(111) by scanning tunneling spectroscopy (STS).[14, 15, 30, 34-38] For eGNRs, the STS data are currently available only for nanoribbons deposited on a semiconductor H:Si(100) substrate, which could not be directly compared to the bandgaps measured for other ribbons on Au(111) as these two substrates have different polarization effects on GNR bandgaps.[34]

Here, we demonstrate that eGNRs can be synthesized on Au(111) following the general procedure shown in Fig. 1b. The ribbons were characterized by scanning tunneling microscopy (STM) and noncontact atomic force microscopy (nc-AFM), both of which confirmed high structural quality of the on-surface synthesized eGNRs. The ribbons were also characterized by STS, which revealed that eGNRs on Au(111) exhibit a bandgap of about 2.2 eV. We compare STS data for eGNRs and cGNRs on Au(111) and demonstrate that the lateral extension of the chevron GNR results in its bandgap reduction.

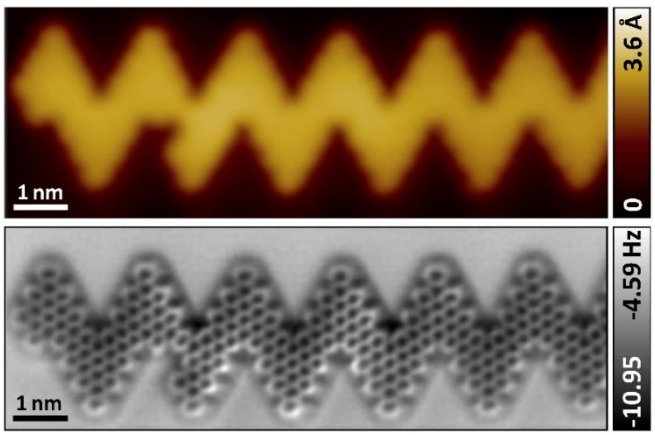

Figure 2. Microscopic characterization of eGNRs. STM (top) and nc-AFM (bottom) images of eGNR on Au(111). STM image scan parameters: 0.1 V, 10 pA.

The molecular precursor **1** was synthesized according to the previously reported procedure.[5] Growth and characterization of eGNRs were performed using an upgraded Createc based LT-STM system with custom GXSM control hardware and software.[39] Prior to the growth, an Au(111) substrate was cleaned by three Ar^+ sputtering/annealing cycles. The molecular precursor **1** was sublimed in UHV onto an Au(111) substrate, which was kept at 4.5 K, using a home-built evaporator. After the molecular depostion, the substrate was heated up to 200 °C for 10 minutes to form polymer **P1** and then to 400 °C for 10 minutes to produce eGNRs. The ribbons on Au(111) were visualized using STM and nc-AFM at 4.5 K. The nc-AFM imaging was performed using a CuO terminated tip[40] at a 50-150 mV STM bias, with a typical tip oscillation amplitude of 50-80 pm and a Q-Plus [© F. Giessibl] sensor operated around 30 kHz.

We performed the growth at a low coverage of molecular precursors to avoid fused GNR structures[37, 41-43] and produce isolated nanoribbons for the STS characterization. STM and nc-AFM images of a representative eGNR on Au(111) are shown in Fig. 2. The images demonstrate that the nanoribbon was synthesized with atomic precision and has a structure that matches the molecular model in Fig. 1a. Only one structural defect could be observed, which originates from missing one of the 1,4-phenyls directly connected to the triphenylene base of the molecular precursor **1** (Fig. 1b). We previously reported that the absent benzene rings associated with the cleavage of the 1,4-phenyls, likely after the polymerization stage, are the most common structural defects in the on-surface synthesized cGNRs and eGNRs.[33] In the STM image, the GNR had an apparent height of about 2.2 to 2.5 Å depending on whether the measurements were taken at the ribbon's edge or center, respectively (see the top panel in Fig. 2); STM heights of about 2 Å were previously reported for other on-surface grown GNRs as well.[19]

Fig. 3 displays STS spectra of eGNRs on Au(111). The red spectrum in Fig. 3a is an average of 20 STS point spectra measured at the edges of several eGNRs on the substrate; a representative edge position used for acquiring spectra of this kind is shown by the black and red crosses in the STM image of eGNR in the inset in Fig. 3a. This STM image also shows a ribbon that nucleated at the step edge on the Au(111) visible in the bottom left part of the inset. An STS point spectrum measured over the bare Au(111) is shown as a reference, demonstrating small peaks in the 0 to -0.5 V range corresponding to the gold surface states.

The spectrum in Fig. 3a shows the dI/dV spectral features that we interpret as the edges of the valence band (VB) and conduction band (CB), respectively. Since these are not well-resolved peaks but rather step-like features, we determined the energies of the corresponding frontier states at 80% of the step rises, as rationalized in ref. [44]. This analysis yielded the VB edge at about -0.7 eV and the CB edge at about 1.5 eV, resulting in the bandgap of 2.2 ± 0.1 eV. These VB and CB edge positions are marked by the dashed maroon lines in Fig. 3a.

While the VB and CB features were generally better resolved in the STS spectra taken at the edges of eGNRs, they were also visible in the spectra taken at various other points within the ribbons. This is illustrated by Fig. 3b, which shows series of spectra taken at the points marked by crosses in the inset in Fig. 3a; the color of each cross (Fig. 3a) corresponds to the color of the spectrum for that location (Fig. 3b). The spectral features at

about -0.7 eV (VB edge) and about 1.5 eV (CB edge) are omnipresent, although their clarity vary from spectrum to spectrum.

Fig. 3c provides a heat-map representation of the STS data shown in Fig. 3b, where the intensity of the dI/dV signal is shown as a function of both the sample bias and the tip position across the eGNR along the line marked by crosses in the inset in Fig. 3a. To aid in visualization of the magnitude of the gap, the region of the graph beyond -0.3 V was multiplied by 2.[30] In this figure, the low-dI/dV points are darker, the higher-dI/dV points are lighter, and the sharp dI/dV transitions corresponding to the VB and CB edges are indicated.

Density functional theory (DFT) calculations predict that the lateral extension of the chevron GNR results in the bandgap reduction from 1.61 eV (cGNR) to 1.38 eV (eGNR).[5, 45] When implementing the *GW* correction, which is known for more accurate prediction of GNR bandgaps,[7, 34] the quasiparticle bandgap of eGNR (3.38 eV) is also found to be smaller than that of cGNR (3.78 eV).[5]

The data presented in Fig. 3 could be directly compared with the results of prior STS studies of cGNRs grown on Au(111).[30, 46] These studies reported that cGNRs on Au(111) exhibit the VB edge at about -0.8 eV and the CB edge at about 1.6-1.7 eV, resulting in the bandgap of about 2.4-2.5 eV.[30, 46] Thus, the STS data for eGNRs on Au(111) with the VB edge at about -0.7 eV, the CB edge at about 1.5 eV, and the bandgap of 2.2 ± 0.1 eV are consistent with the theoretically predicted bandgap reduction upon the lateral extension of cGNRs to eGNRs.[5]

It has been well established that in the STS measurements of GNRs the bandgaps are reduced compared to the expected values for free-standing ribbons in vacuum due to the substrate polarization effect.[34] For example, while cGNRs show a bandgap of 2.4-2.5 eV on Au(111),[30, 46] when studied by STS on a semiconducting H:Si(100) substrates they exhibit a larger bandgap of about 2.8 eV because of the reduced effect of the substrate polarization.[32] Likewise, the ~2.2. eV bandgap measured in this study for eGNRs on Au(111) is consistently smaller than 2.66 eV determined in the prior STS study of the solution-synthesized eGNRs that were deposited on H:Si(100).[5] Thus, the results of STS studies of eGNRs on Au(111) are consistent with theory and prior investigations of cGNRs and eGNRs on various substrates.

In summary, we demonstrated the on-surface synthesis of eGNRs on Au(111) *via* polymerization of molecule **1** at 200 °C and cyclodehydrogenation of the resulting polymer at 400 °C. The high structural quality of eGNRs was confirmed by microscopic techniques, including STM and nc-AFM. The ribbons were also characterized by STS, which revealed that eGNRs on Au(111) exhibit a bandgap of about 2.2 ± 0.1 eV. The bandgap value and the placement of VB and CB edges are consistent with the theoretically predicted bandgap reduction upon the lateral extension of cGNRs to eGNRs, as well as with previously reported STS data for cGNRs on Au(111). Further, the magnitude of the bandgap is confirmed to be consistent as a function of position across the eGNR. Considering that most other GNRs reported so far have been characterized by STS on Au(111),[14, 15, 30, 34-38] eGNRs can now be directly compared to other established nanoribbons in terms of their electronic properties. In particular, this information could be useful for designing new GNR

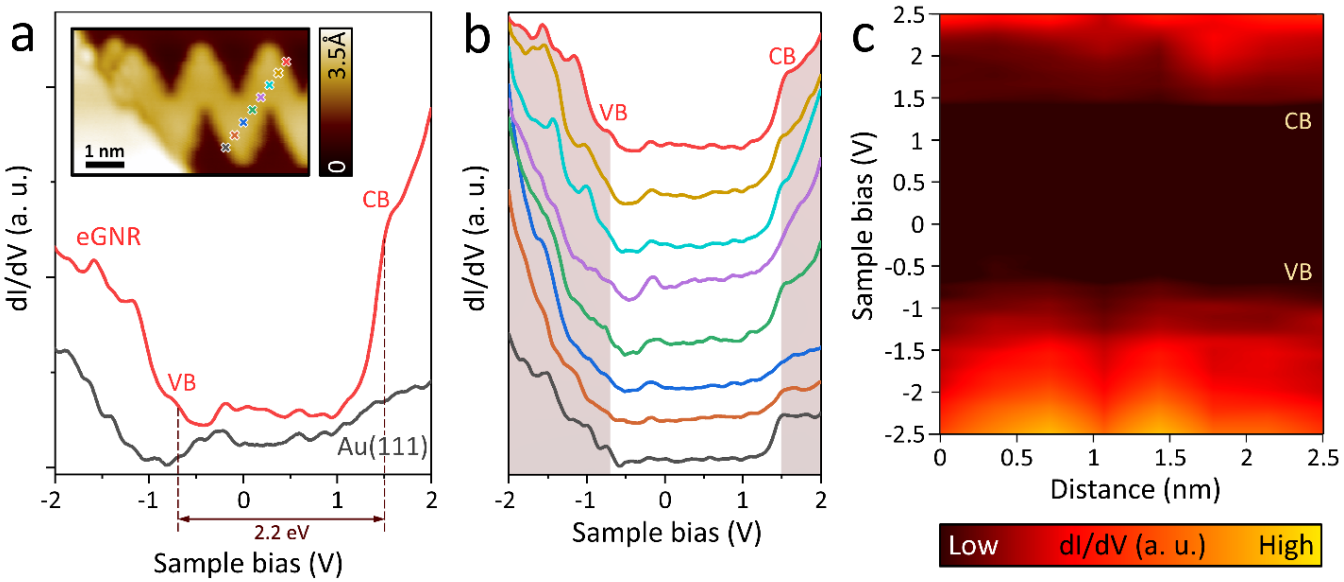

Figure 3. STS characterization of eGNRs. (a) STS dI/dV spectra of an eGNR on Au(111) and bare Au(111) substrate, which is provided as a reference. The spectrum of the eGNR was averaged over 20 dI/dV point spectra acquired at the edges of several ribbons. The inset shows an STM image of a fragment of eGNR with the crosses indicating points at which the STS spectra were collected. STM image scan parameters: 0.2 V, 10 pA. (b) Stacked line cut of spectra across an eGNR; points of collection of the spectra correspond to the colors of the crosses indicated in the inset. The VB and CB edges are most clearly defined at the edges of the eGNR, and points outside these are shadowed in grey to highlight the band gap. (c) Heat-map visualization of the data in panel (b). Darker regions of the graph represent low dI/dV values, and brighter regions correspond to higher values. The valence-band portion of the graph, beyond -0.3V, is multiplied by 2 to more appropriately highlight the VB edge.

heterojunctions, in which eGNR units would be combined with fragments of other GNRs.[26, 30, 33, 35]

Acknowledgements

The work was supported by the Office of Naval Research (N00014-16-1-2899) and the National Science Foundation (CHE-1455330). This research used resources of the Center for Functional Nanomaterials, which is a U.S. DOE Office of Science Facility, at Brookhaven National Laboratory under Contract No. DE-SC0012704.

Conflict of Interest

The authors declare no conflict of interest.

Keywords: graphene nanoribbons • on-surface synthesis • scanning tunneling microscopy • scanning tunneling spectroscopy • noncontact atomic force microscopy

[1] J. P. Llinas, A. Fairbrother, G. Borin Barin, W. Shi, K. Lee, S. Wu, B. Yong Choi, R. Braganza, J. Lear, N. Kau, W. Choi, C. Chen, Z. Pedramrazi, T. Dumslaff, A. Narita, X. Feng, K. Müllen, F. Fischer, A. Zettl, P. Ruffieux, E. Yablonovitch, M. Crommie, R. Fasel, J. Bokor, *Nat. Commun.* **2017**, *8*, 633.

[2] Y.-W. Son, M. L. Cohen, S. G. Louie, *Nature* **2006**, *444*, 347-349.

[3] S. Osella, A. Narita, M. G. Schwab, Y. Hernandez, X. L. Feng, K. Müllen, D. Beljonne, *ACS Nano* **2012**, *6*, 5539-5548.

[4] E. Castro, T. J. Sisto, E. L. Romero, F. Liu, S. R. Peurifoy, J. Wang, X. Zhu, C. Nuckolls, L. Echegoyen, *Angewandte Chemie International Edition* **2017**, *56*, 14648-14652.

[5] M. Mehdi Pour, A. Lashkov, A. Radocea, X. Liu, T. Sun, A. Lipatov, R. A. Korlacki, M. Shekhirev, N. R. Aluru, J. W. Lyding, V. Sysoev, A. Sinitskii, *Nat. Commun.* **2017**, *8*, 820.

[6] K. Nakada, M. Fujita, G. Dresselhaus, M. S. Dresselhaus, *Phys. Rev. B* **1996**, *54*, 17954-17961.

[7] L. Yang, C.-H. Park, Y.-W. Son, M. L. Cohen, S. G. Louie, *Phys. Rev. Lett.* **2007**, *99*, 186801.

[8] V. Barone, O. Hod, G. E. Scuseria, *Nano Lett.* **2006**, *6*, 2748-2754.

[9] M. Fujita, K. Wakabayashi, K. Nakada, K. Kusakabe, *J. Phys. Soc. Jpn.* **1996**, *65*, 1920-1923.

[10] W. Y. Kim, K. S. Kim, *Nat. Nanotechnol.* **2008**, *3*, 408-412.

[11] T. Cao, F. Zhao, S. G. Louie, *Phys. Rev. Lett.* **2017**, *119*, 076401.

[12] L. Talirz, P. Ruffieux, R. Fasel, *Adv. Mater.* **2016**, *28*, 6222-6231.

[13] A. Narita, X.-Y. Wang, X. Feng, K. Müllen, *Chem. Soc. Rev.* **2015**, *44*, 6616-6643.

[14] Y.-C. Chen, D. G. de Oteyza, Z. Pedramrazi, C. Chen, F. R. Fischer, M. F. Crommie, *ACS Nano* **2013**, *7*, 6123-6128.

[15] A. Kimouche, M. M. Ervasti, R. Drost, S. Halonen, A. Harju, P. M. Joensuu, J. Sainio, P. Liljeroth, *Nat Commun*. **2015**, *6*, 10177.

[16] P. Ruffieux, S. Wang, B. Yang, C. Sánchez-Sánchez, J. Liu, T. Dienel, L. Talirz, P. Shinde, C. A. Pignedoli, D. Passerone, T. Dumslaff, X. Feng, K. Müllen, R. Fasel, *Nature* **2016**, *531*, 489-492.

[17] O. Gröning, S. Wang, X. Yao, C. A. Pignedoli, G. Borin Barin, C. Daniels, A. Cupo, V. Meunier, X. Feng, A. Narita, K. Müllen, P. Ruffieux, R. Fasel, *Nature* **2018**, *560*, 209-213.

[18] D. J. Rizzo, G. Veber, T. Cao, C. Bronner, T. Chen, F. Zhao, H. Rodriguez, S. G. Louie, M. F. Crommie, F. R. Fischer, *Nature* **2018**, *560*, 204-208.

[19] J. M. Cai, P. Ruffieux, R. Jaafar, M. Bieri, T. Braun, S. Blankenburg, M. Muoth, A. P. Seitsonen, M. Saleh, X. L. Feng, K. Müllen, R. Fasel, *Nature* **2010**, *466*, 470-473.

[20] J. D. Teeter, P. S. Costa, M. Mehdi Pour, D. P. Miller, E. Zurek, A. Enders, A. Sinitskii, *Chem. Commun.* **2017**, *53*, 8463-8466.

[21] T. H. Vo, M. Shekhirev, D. A. Kunkel, M. D. Morton, E. Berglund, L. M. Kong, P. M. Wilson, P. A. Dowben, A. Enders, A. Sinitskii, *Nat. Commun.* **2014**, *5*, 3189.

[22] T. H. Vo, M. Shekhirev, A. Lipatov, R. A. Korlacki, A. Sinitskii, *Faraday Discussions* **2014**, *173*, 105-113.

[23] C. Bronner, S. Stremlau, M. Gille, F. Brauße, A. Haase, S. Hecht, P. Tegeder, *Angewandte Chemie International Edition* **2013**, *52*, 4422-4425.

[24] T. H. Vo, M. Shekhirev, D. A. Kunkel, F. Orange, M. J. F. Guinel, A. Enders, A. Sinitskii, *Chem. Commun.* **2014**, *50*, 4172-4174.

[25] Y. Zhang, Y. Zhang, G. Li, J. Lu, X. Lin, S. Du, R. Berger, X. Feng, K. Müllen, H.-J. Gao, *Appl. Phys. Lett.* **2014**, *105*, 023101.

[26] J. Cai, C. A. Pignedoli, L. Talirz, P. Ruffieux, H. Söde, L. Liang, V. Meunier, R. Berger, R. Li, X. Feng, K. Müllen, R. Fasel, *Nat. Nanotechnol.* **2014**, *9*, 896-900.

[27] T. H. Vo, U. G. E. Perera, M. Shekhirev, M. Mehdi Pour, D. A. Kunkel, H. Lu, A. Gruverman, E. Sutter, M. Cotlet, D. Nykypanchuk, P. Zahl, A. Enders, A. Sinitskii, P. Sutter, *Nano Lett.* **2015**, *15*, 5770-5777.

[28] T. Marangoni, D. Haberer, D. J. Rizzo, R. R. Cloke, F. R. Fischer, *Chemistry – A European Journal* **2016**, *22*, 13037-13040.

[29] Y.-F. Zhang, Y. Zhang, G. Li, J. Lu, Y. Que, H. Chen, R. Berger, X. Feng, K. Müllen, X. Lin, Y.-Y. Zhang, S. Du, S. T. Pantelides, H.-J. Gao, *Nano Res.* **2017**, *10*, 3377-3384.

[30] G. D. Nguyen, H.-Z. Tsai, A. A. Omrani, T. Marangoni, M. Wu, D. J. Rizzo, G. F. Rodgers, R. R. Cloke, R. A. Durr, Y. Sakai, F. Liou, A. S. Aikawa, J. R. Chelikowsky, S. G. Louie, F. R. Fischer, M. F. Crommie, *Nat. Nanotechnol.* **2017**, *12*, 1077-1081.

[31] M. Shekhirev, P. Zahl, A. Sinitskii, *ACS Nano* **2018**, *12*, 8662–8669.

[32] A. Radocea, T. Sun, T. H. Vo, A. Sinitskii, N. R. Aluru, J. W. Lyding, *Nano Lett.* **2017**, *17*, 170-178.

[33] P. S. Costa, J. D. Teeter, A. Enders, A. Sinitskii, *Carbon* **2018**, *134*, 310-315.

[34] P. Ruffieux, J. Cai, N. C. Plumb, L. Patthey, D. Prezzi, A. Ferretti, E. Molinari, X. Feng, K. Müllen, C. A. Pignedoli, R. Fasel, *ACS Nano* **2012**, *6*, 6930-6935.

[35] Y.-C. Chen, T. Cao, C. Chen, Z. Pedramrazi, D. Haberer, D. de Oteyza, G., F. R. Fischer, S. G. Louie, M. F. Crommie, *Nat. Nanotechnol.* **2015**, *10*, 156-160.

[36] L. Talirz, H. Söde, T. Dumslaff, S. Wang, J. R. Sanchez-Valencia, J. Liu, P. Shinde, C. A. Pignedoli, L. Liang, V. Meunier, N. C. Plumb, M. Shi, X. Feng, A. Narita, K. Müllen, R. Fasel, P. Ruffieux, *ACS Nano* **2017**, *11*, 1380-1388.

[37] N. Merino-Díez, A. Garcia-Lekue, E. Carbonell-Sanromà, J. Li, M. Corso, L. Colazzo, F. Sedona, D. Sánchez-Portal, J. I. Pascual, D. G. de Oteyza, *ACS Nano* **2017**, *11*, 11661-11668.

[38] N. Merino-Díez, J. Li, A. Garcia-Lekue, G. Vasseur, M. Vilas-Varela, E. Carbonell-Sanromà, M. Corso, J. E. Ortega, D. Peña, J. I. Pascual, D. G. de Oteyza, *The Journal of Physical Chemistry Letters* **2018**, *9*, 25-30.

[39] P. Zahl, T. Wagner, *Imaging and Microscopy* **2015**, *17*, 38-41.

[40] H. Mönig, D. R. Hermoso, O. Díaz Arado, M. Todorović, A. Timmer, S. Schüer, G. Langewisch, R. Pérez, H. Fuchs, *ACS Nano* **2016**, *10*, 1201-1209.

[41] H. Huang, D. Wei, J. Sun, S. L. Wong, Y. P. Feng, A. H. Castro Neto, A. T. S. Wee, *Sci Rep.* **2012**, *2*, 983.

[42] J. D. Teeter, P. S. Costa, P. Zahl, T. H. Vo, M. Shekhirev, W. Xu, X. C. Zeng, A. Enders, A. Sinitskii, *Nanoscale* **2017**, *9*, 18835-18844.

[43] C. Ma, L. Liang, Z. Xiao, A. A. Puretzky, K. Hong, W. Lu, V. Meunier, J. Bernholc, A.-P. Li, *Nano Lett.* **2017**, *17*, 6241-6247.

[44] H. Söde, L. Talirz, O. Gröning, C. A. Pignedoli, R. Berger, X. Feng, K. Müllen, R. Fasel, P. Ruffieux, *Phys. Rev. B* **2015**, *91*, 045429.

[45] Y.-L. Lee, F. Zhao, T. Cao, J. Ihm, S. G. Louie, *Nano Lett.* **2018**, *18*, 7247-7253.

[46] O. Deniz, C. Sanchez-Sanchez, R. Jaafar, N. Kharche, L. Liang, V. Meunier, X. Feng, K. Müllen, R. Fasel, P. Ruffieux, *Chem. Commun.* **2018**, *54*, 1619-1622.

Entry for the Table of Contents

COMMUNICATION

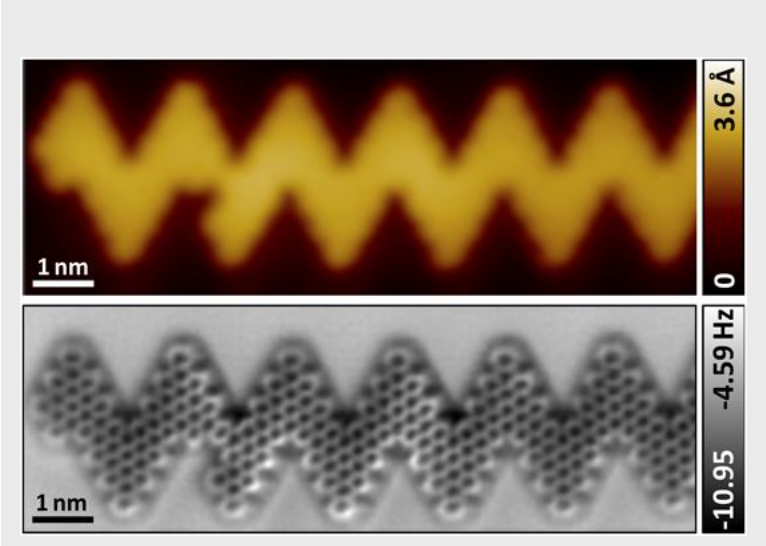

*Jacob D. Teeter, Percy Zahl, Mohammad Mehdi Pour, Paulo S. Costa, Axel Enders, Alexander Sinitskii**

Page No. – Page No.

On-surface synthesis and spectroscopic characterization of laterally extended chevron graphene nanoribbons

Graphene nanoribbons: Reported is the on-surface synthesis and spectroscopic study of laterally extended chevron graphene nanoribbons (GNRs). The extended chevron GNRs grown on Au(111) exhibit a bandgap of about 2.2 eV, which is considerably smaller than the values reported for the established chevron GNRs in similar studies.